HHS Public Access

Author manuscript

J Neurochem. Author manuscript; available in PMC 2022 March 01.

Published in final edited form as:

J Neurochem. 2021 March ; 156(5): 589–603. doi:10.1111/jnc.14990.

Reelin signaling modulates $GABA_B$ receptor function in the neocortex

Mohammad I.K. Hamad[1,2], **Abdalrahim Jbara**[1], **Obada Rabaya**[1], **Petya Petrova**[1], **Solieman Daoud**[1], **Nesrine Melliti**[1], **Maurice Meseke**[1], **David Lutz**[1], **Elisabeth Petrasch-Parwez**[1], **Jan Claudius Schwitalla**[3], **Melanie D. Mark**[3], **Stefan Herlitze**[4], **Gebhard Reiss**[2], **Joachim Herz**[5], **Eckart Förster**[1]

[1]Department of Neuroanatomy and Molecular Brain Research, Ruhr University Bochum, Medical Faculty, Bochum, Germany

[2]Institute for Anatomy and Clinical Morphology, School of Medicine, Faculty of Health, Witten/Herdecke University, Witten, Germany

[3]Department of Behavioral Neuroscience, Ruhr University Bochum, Bochum, Germany

[4]Department of Zoology and Neurobiology, Ruhr University Bochum, Bochum, Germany

[5]Departments of Molecular Genetics, Neuroscience, Neurology and Neurotherapeutics; Center for Translational Neurodegeneration Research, University of Texas Southwestern Medical Center, Dallas, Texas, USA

Abstract

Reelin is a protein that is best known for its role in controlling neuronal layer formation in the developing cortex. Here, we studied its role for postnatal cortical network function, which is poorly explored. To preclude early cortical migration defects caused by Reelin deficiency, we used a conditional Reelin knock-out ($Reln^{cKO}$) mouse, and induced Reelin deficiency postnatally. Induced Reelin deficiency caused hyperexcitability of the neocortical network *in vitro* and *ex-vivo*. Blocking Reelin binding to its receptors ApoER2 and VLDLR resulted in a similar effect. Hyperexcitability in $Reln^{cKO}$ organotypic slice cultures (OTCs) could be rescued by co-culture with wildtype OTCs. Moreover, the $GABA_B$ receptor ($GABA_BR$) agonist baclofen failed to activate and the antagonist CGP35348 failed to block $GABA_B$Rs in $Reln^{cKO}$ mice. Immunolabelling of $Reln^{cKO}$ cortical slices revealed a reduction in $GABA_BR1$ and $GABA_BR2$ surface expression at the plasma membrane and western blot of $Reln^{cKO}$ cortical tissue revealed decreased phosphorylation of the $GABA_BR2$ subunit at serine 892 and increased phosphorylation at serine 783, reflecting receptor deactivation and proteolysis. These data show a role of Reelin in controlling early network activity, by modulating $GABA_BR$ function.

Graphical Abstract

Correspondence: mohammad.hamad@uni-wh.de (M.I.K.H.), eckart.foerster@rub.de (E.F.).

Competing interests: The authors declare that they have no competing interests.

Data and materials availability: The $Reln^{cKO}$ mice require a material transfer agreement from the University of Texas Southwestern Medical Center.

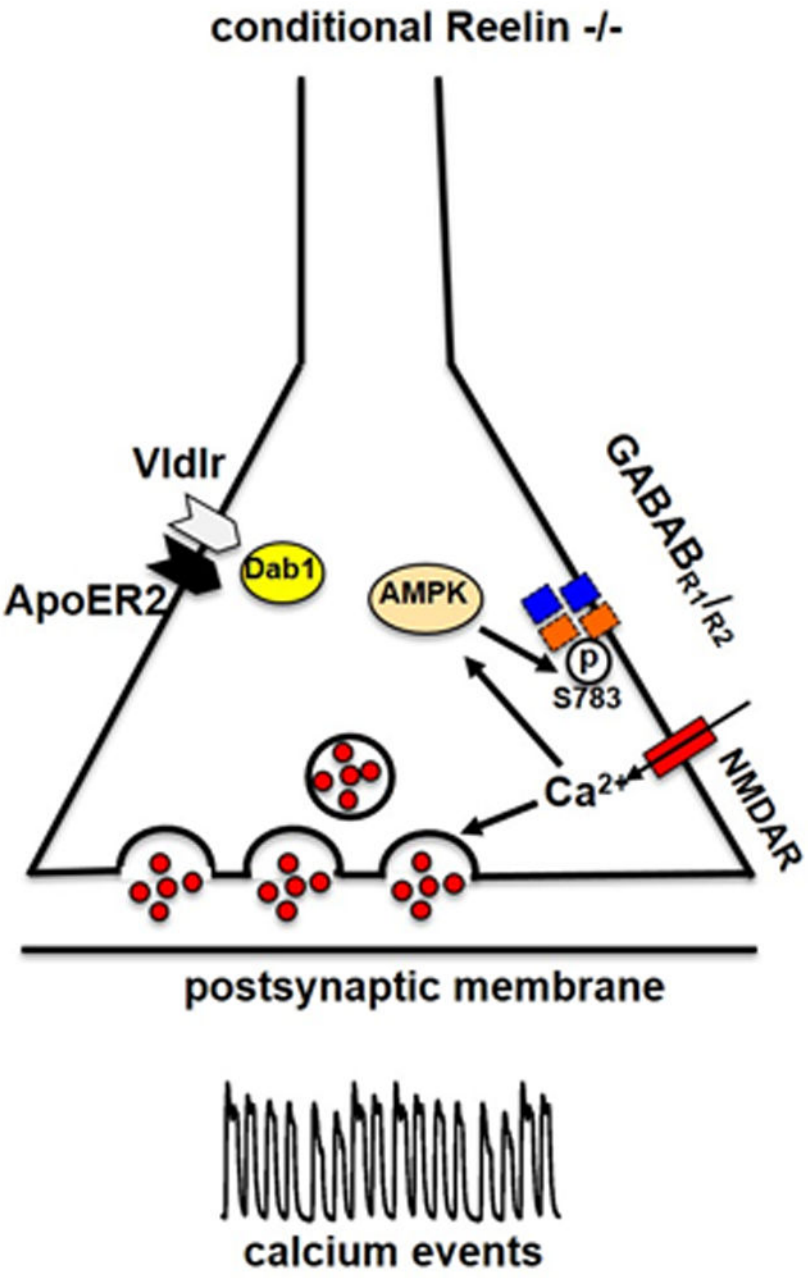

We suggested the following modification of synaptic function after conditional reelin knockout in the cerebral cortex: After Reelin deficiency, the presynaptic reelin signaling cascade via the reelin receptors ApoER2 and Vldlr and the adaptor protein Dab1, is no longer activated. This causes a decreased phosphorylation of presynaptic $GABA_B$-receptors at S892, while phosphorylation at S783 increases, likely induced by AMP-activated protein kinase (AMPK). As a consequence, $GABA_B$-receptors are degraded, calcium influx via NMDA-receptors and synaptic vesicle release is increased. We believe that our findings revealed a new synaptic function of reelin expressed by cortical interneurons during cortical development.

Introduction

Reelin is an extracellular glycoprotein that controls several aspects of mammalian brain development and function. The most prominent role of Reelin is the control of neuronal migration and layer formation in the developing cerebral cortex, as evidenced by numerous histological studies on reeler mutant mice that lack Reelin expression due to a defect of the Reelin gene (Caviness 1976; Curran and D'Arcangelo 1998; Lambert de Rouvroit and Goffinet 1998). Through signaling via its membrane receptors (Bock and May 2016; Cooper and Howell 1999), Reelin guides the migration of newborn neurons and orchestrates the development of cortical layers. In the developing and adult brain, the majority of GABAergic interneurons in the neocortex expresses Reelin. The canonical Reelin signaling cascade involves direct binding of Reelin to ApoER2 and VLDLR and subsequent activation of the intracellular adapter protein Disabled-1 (DAB1) by tyrosine phosphorylation (Cooper and Howell 1999; D'Arcangelo et al. 1999; Hiesberger et al. 1999; Howell et al. 2000; Trommsdorff et al. 1999).

In the absence of Reelin or its receptors, the process of neuronal migration is compromised, which causes severe abnormalities in cortical lamination. The resulting phenotype was initially described as an inversion of the layers (Caviness 1982; Caviness and Sidman 1973). Although it had already been shown that deviant barrel formation in the somatosensory cortex of the reeler is compromised (Caviness 1976; Welt and Steindler 1977), it has been recently demonstrated that the barrel field retains its proper somatotopic organization (Guy et al. 2015; Wagener et al. 2010). Besides its cortical migration defects, the reeler mutants exhibit cerebellar hypoplasia and a neurological phenotype that is characterized by ataxia ((Miyata et al. 1997). A similar phenotype was observed in human patients carrying homozygous mutations in the Reelin gene, resulting in lissencephaly and cerebellar hypoplasia (Hong et al. 2000). Moreover, in humans, heterozygous Reelin mutations were described that cause autosomal-dominant temporal lobe epilepsy (Dazzo et al. 2015).

Gamma-aminobutyric acid (GABA) is the major inhibitory neurotransmitter in the mammalian CNS and plays a key role in modulating neuronal activity. GABA mediates its action via two different classes of receptors, ionotropic receptors ($GABA_A$, $GABA_C$) and metabotropic $GABA_B$ receptors. The $GABA_B$ receptors are guanine nucleotide-binding protein (G protein)-coupled metabotropic receptors that modulate Ca^{2+}- and potassium (K^+) – channels, and elicit both presynaptic and slow postsynaptic inhibition (Benarroch 2012; Bettler et al. 2004). In particular, presynaptic $GABA_B$Rs are coupled to Ca^{2+} channels, regulating the release of neurotransmitters, while postsynaptic $GABA_B$Rs are coupled to K^+ inward rectifying (Kir) channels (Kir3), regulating postsynaptic slow inhibition (Pinard et al. 2010). Remarkably, GABA does not mediate hyperpolarization-dependent inhibition during early development, since $GABA_A$R signaling is mainly depolarizing and excitatory during this period, while $GABA_B$Rs are uncoupled from G-proteins and Kir3 channels until the end of the first postnatal week (Ben-Ari et al. 2012; Fukuda et al. 1993; Owens and Kriegstein 2002). Moreover, GABA is abundant in the neonatal nervous system and activates $GABA_B$Rs (Ben-Ari et al. 2007). In the cortex, $GABA_B$R1 and $GABA_B$R2 were detected by immunocytochemistry as early as E14, and $GABA_{B1}$Rs were found to colocalize with $GABA_{B2}$Rs in neurons of the marginal zone and the subplate, indicating that these proteins

are coexpressed and could be forming functional $GABA_BRs$ during prenatal development *in vivo* (López-Bendito et al. 2002). In the murine neocortex, Reelin-haploinsufficiency has been shown to disrupt the developmental trajectory of GABA excitation/inhibition balance (Bouamrane et al. 2016), suggesting a possible interaction between Reelin and the GABA receptors.

Adult conditionally induced $Reln^{cKO}$ mice exhibited altered hippocampal LTP and a subtle behavioural phenotype while the cortical architecture was shown to be indistinguishable from their wild-type littermate (Lane-Donovan et al. 2015). The question whether Reelin deficiency affects early cortical neuronal activity remains to be solved. To address this question, we investigated the effect of postnatally induced Reelin deficiency on Ca^{2+} signaling and on synaptic function in the neocortex of $Reln^{cKO}$ mice. Since synaptic release is mainly controlled by $GABA_BRs$ that mediate inhibitory GABA effects around the second postnatal week, we focused here on a potential interaction between Reelin signaling and $GABA_BRs$ function.

Material and Methods

Reelin conditional knockout mice ($Reln^{cKO}$)

Animals were housed in a standard 12-h light cycle and fed ad libitum with standard mouse chow. All care and use of experimental animals were respected according to the Federal German law with permission Nr. 84-02.04.2016.A383 and the ARRIVE guidelines. The generation of the conditional $Reln^{cKO}$ line was previously described (Lane-Donovan et al. 2015). To obtain conditional Reelin knockout mice ($Reln^{flox/flox}$ CAG-Cre^{ERT2} mice), we crossed $Reln^{flox/flox}$ mice with hemizygous tamoxifen-inducible Cre recombinase expressing mice (CAG-Cre^{ERT2}) (Hayashi and McMahon 2002). For the experiments, only $Reln^{flox/flox}$ CAG-Cre^{ERT2} male mice were selected and then crossed with $Reln^{flox/flox}$ female mice to generate $Reln^{flox/flox\ wildtype}$ (WT) and $Reln^{flox/flox}$ CAG-Cre^{ERT2} ($Reln^{cKO}$) siblings as verified by PCR. The cKO mouse line ubiquitously expresses a fusion protein comprising Cre recombinase and a mutated form of the estrogen receptor (Cre-ERT2). Tamoxifen administration induces nuclear Cre activation and knockout of the floxed Reelin gene. 20 μl tamoxifen (Cat# T5648, Sigma, Deisenhofen, Germany) was dissolved in corn oil at a concentration of 20 mg/ml by shaking overnight at 37°C and fed to newly born pups at P1 for 5 consecutive days. At P14 animals were deep anesthetized with isoflurane CP® (CP-Pharma, Burgdorf, Germany) to minimize suffering and killed by decapitation. Ex-vivo slices from somatosensory cortex were explanted from each animal for acute slice preparation at P14 or at P0 for OTCs preparation by respecting the coordinates indicated in Allens mouse brain atlas. A graphical flow chart for ex-vivo experimental procedures is shown in (Fig. 1A). For each outcome measure, we used 5 $Reln^{wt}$ and 5 $Reln^{cKO}$ mice (each experiment was repeated 3 times). In total 390 animals were used for this study. From each animal we obtained 3-4 slices. We recorded from each slice 3 different areas of interests (ROI). In each area of interest, we averaged amplitude, frequency and Ca^{2+} transient half-width of 6 cells. The average of the 3 ROI has been plotted in the box-plot as single value. This study was not pre-registered. No exclusion criteria were pre-determined and the study

was exploratory. No blinding, randomization was performed to allocate subjects in the study. No sample size calculation was performed in this study.

PCR and genotyping

All samples were stored at −20°C until PCR analysis. DNA from samples of ear, tail and brain tissue were isolated with ReliaPrep gDNA kit (Cat# A205, Promega, Mannheim, Germany). All procedures were performed according to protocols provided by the manufacturer. The amounts of DNA isolated from the various samples were determined by spectrophotometry with the Genova Nano system (Jenway). DNA was amplified by PCR. PCR reactions were performed in a total volume of 50 µl reaction mixture containing 200 ng of template DNA, Soriano buffer (0.67 M Tris, 0.16 M ammonium sulphate, 67 mM $MgCl_2$, 67 µM EDTA and 50 mM β-Mercaptoethanol), Taq polymerase, 2 µL DMSO and 10 mM dNTPs. For genotyping we used the following primers: Wildtype mice, forward primer 5′-ATAAACTGGTGCTTATGTGACAGG-3′, reverse primer 5′-AGACAATGCTAACAACAGCAAGC-3′ (450 bp). $Reln^{flox/flox}$ mice, forward primer 5′-GCTCTGGCCAAGCTTTATC-3′, reverse primer 5′-CGCGATCGATAACTTCGTATAGCATAC-3′ (1200 bp). For detection of CAG-Cre^{ERT2}, forward primer 5′-ATTGCTGTCACTTGGTCGTGG-3′, reverse primer 5′-GGAAAATGCTTCTGTCCGTTTGC-3′ (200 bp). The amplification products were verified on a 2% agarose gel in TBE buffer.

Organotypic cultures and pharmacological treatment

OTCs were prepared from newborn postnatal day 0 (P0) mice. 3-4 OTCs from somatosensory cortex were collected from each animal. All solutions used for OTCs preparation were sterile and all preparations were performed in a laminar air flow bench with horizontal counter flow (Horizontal Flow, ICN, Biomedicals, Eschwege; Germany). The mice were briefly anesthetized and decapitated. The skull was removed gently, and the cortex was placed on the chopper plate (McIllwain, Bad Schwalbach, Germany). Somatosensory cortex was cut into 350 µm thick slices, and the slices were gently transferred into ice cold buffered salt solution (GBSS, Cat# 24020117, Gibco, Eggenstein, Germany) containing 25 mM D-glucose. After 30 minutes of recovery, the slices were transferred onto coverslips (12 x 24 mm, Kindler). A mixture of chicken plasma (Sigma) and GBBS/thrombin (Merck) was mixed in a proportion of 2:1 and then allowed to coagulate for 45 min. The coverslip was transferred into a roller tube (Nunc) filled with 750 µl semiartificial medium and placed in a roller incubator at 37 °C. To induce the knockout, the OTCs were directly stimulated after preparation with 1 µM (Z)-4-hydroxytamoxifen (4-OHT) (Cat# 3412, Tocris, Wiesbaden, Germany) for 5 consecutive days and kept for experiments until DIV14. A graphical flow chart for OTCs experimental procedures is shown in (Fig. 2A). For the Ca^{2+} imaging experiments, the following drugs were used: Baclofen (10 µM, Cat# 0417, Tocris, Wiesbaden, Germany), CGP35348 (10 µM, Cat# 1245/10, Tocris, Wiesbaden, Germany), PP2 (1 µM, Cat# 1407/10, Tocris, Wiesbaden, Germany), pertussis toxin (PTX, 500 ng/mL, Cat# 3097/50U, Tocris, Wiesbaden, Germany), CNQX (10 µM, Cat# 0190/10, Tocris, Wiesbaden, Germany) and APV (50 µM, Cat# 0190/10, Tocris, Wiesbaden, Germany). As an inhibitor of low-density lipoprotein receptor–related proteins, we used the recombinant Mouse LRPAP Protein (LDL receptor-related

protein-associated protein 1; also named receptor-associated protein (RAP), 50 ng/ml, Cat# 4480-LR, R&D Systems). RAP serves as a molecular chaperone for LDL receptor family proteins including VLDL and APOER2 and prevents interaction of ligands with these receptors. Therefore, RAP is used to block the canonical Reelin pathway by blocking Reelin from binding to VLDL and APOER2 (Bu and Schwartz 1998; Gong et al. 2007; Herz et al. 1991).

Expression plasmids and biolistic transfection

Transfection was performed using a Helios Gene Gun (Bio-Rad) as described previously (Wirth and Wahle 2003). In brief, cartridges were prepared by coating 10 mg gold particles (Ø = 1μm; Bio-Rad) with genetically encoded Ca^{2+} indicator pGP-CMV-GCaMP6s (GCaMP6s). GCaMP6s was a gift from Douglas Kim (RRID: Addgene_40753) (Chen et al. 2013). To prevent excitotoxicity during transfection, glutamate receptors were temporarily blocked with 3 mM kynuric acid (Cat# K3375, Sigma, Deisenhofen, Germany) and 50 mM APV (Cat# A5282, Sigma, Deisenhofen, Germany) before blasting. The blockers were washed out 3 hours after transfection.

Ca^{2+} imaging using Spinning disc laser microscopy

For studying network activity, Ca^{2+} imaging was performed in somatosensory cortex of supragranular layers II/III with the Ca^{2+} indicator Oregon Green BAPTA-1 Acetoxymethyl ester (OGB-1 AM) (Cat# O6807, Molecular Probes, Eugene, OR, USA). Acute slices (P14) or OTCs DIV14 were loaded according to our previously published protocol (Hamad et al. 2015). In brief, a solution of 20% PF127 (Cat# P2443, Sigma, Steinheim, Germany) dissolved in DMSO (w/v) (J.T. Baker) was prepared to dissolve OGB-1 AM. The final loading solution concentration was 1 μM OGB-1 AM. After loading, the slices were washed several times to remove excess dye and allowed to recover for an hour. The slices were then transferred to the recording chamber mounted on a fixed stage of an inverted microscope, and perfused with 95% O_2, 5% CO_2-bubbled artificial cerebrospinal fluid (ACSF; 3–5 ml/min) at 32 ± 2 °C. Composition of ACSF: (125 mM NaCl, 5 mM KCl, 2 mM $CaCl_2$, 1 mM $MgSO_4$, 25 mM $NaHCO_3$, 1.25 mM NaH2PO4, 25 mM glucose, pH 7.4). The osmolality was 295±5 mOsm as determined with a cryoscopic osmometer (Osmomat 030, Gonotec, Berlin, Germany). Fluorometric Ca^{2+}-recordings were made using a Visiscope spinning-disc confocal system CSU-W1 (Visitron, Munich, Germany) featuring a spinning disk unit CSU-W1-T2 and a sCMOS digital scientific grade camera (4.2 Mpixel rolling shutter version) on an inverted Nikon Ti-E motorized microscope using a CFI P-Fluor 20× objective (NA 0.5, WD = 2.10 mm). Images were acquired at 3 frames per second with exposure times of 330 ms with VisiView image acquisition software (Visitron, Munich, Germany). The Ca^{2+} dye OGB-1 AM and the biosensor GCaMP6s were excited at 488 nm. Emitted fluorescence was collected through ET 525/50 filter for OGB-1 AM and GCaMP6s. Fluorometric data are expressed as $\Delta F/F^0$ (background-corrected increase in fluorescence divided by the resting fluorescence). Raw data delivered in the form of a linear 16-bit intensity scale were plotted as fluorescence intensity versus time. Pyramidal cell or interneuron somata were chosen as the region of interest (ROI). The background fluorescence measured near a ROI was then subtracted from these raw data. The baseline fluorescence (F^0) was calculated as an average of 20 frames in a time window without neuronal activity (as judged by visual inspection).

Subsequently, data were normalized to the mean fluorescence intensities [$\Delta F/F^0 = (F–F^0)/F^0$], allowing the comparison of data across experiments. Spike (calcium transient) half-width was calculated as the width of the spike at half-maximal amplitude (Weir et al. 2014).

Immunohistochemistry and surface labelling

At DIV10, OTCs were fixed with 4% paraformaldehyde (PFA) in 0.1 M phosphate buffer pH 7.4 and warmed to 36°C for 1 hour. After washing twice in TBS (Tris buffered Saline: 50 mM Tris, 150 mM NaCl, pH 7.6) and permeabilization in TBST (TBS, 0.1% Triton X), OTCs were blocked for 1 hour with 1% normal goat serum in TBST. Primary antibodies diluted in TBST were incubated for 24 h at room temperature. The following antibodies were used: Mouse anti-Reelin G10 (Cat# MAB5364, RRID: AB_2179313, 1:1000) , rabbit anti-Cre recombinase (Cat# 69050 , RRID: AB_2314229, 1:2000), rabbit anti-Cux-1 (CULT-1, Cat# ab140042, Abcam, Cambridge, UK, 1:500), rabbit anti-Wolframin 1 (WFS 1, Cat# 11558-1-AP, RRID: AB_2216046, 1:2000), mouse anti-Parvalbumin (Parv, Cat# 235, RRID: AB_10000343, 1:3000), rabbit anti-Glutamate Decarboxylase-65 (GAD65, Cat# G5038, RRID: AB_259920, 1:1000). After washing twice in TBS, the secondary antibodies were added accordingly: Goat anti mouse or goat anti rabbit biotinylated (Cat# E043201-8, Dako, Hamburg, Germany, 1:300). After several washes in TBS buffer, the slices were subjected to ABC-horseradish peroxidase method using diaminobenzidine as chromogen. For immunofluorescence, the slices were subsequently washed 3 × 15 min with TBST and incubated with secondary antibodies (anti-mouse IgG coupled to Alexa594 and anti-rabbit IgG coupled to Alexa488 in TBS (ThermoFisher, Darmstadt, Germany, 1:300) for 30 min at room temperature. After three repetitive washings with TBS-Tween, the OTCs were mounted with sRIMS mounting medium (70% sorbitol w/v in 0.02 M phosphate buffer with 0.01% sodium azide, pH 7.5). Fluorescence was analysed with the Visiscope spinning-disc confocal system as mentioned above. For $GABA_BR1$ und $GABA_BR2$ surface labelling, P14 wt and $Reln^{cKO}$ acute slices were fixed with 4% paraformaldehyde. After several washes in TBS, a group of acute slices was permeabilized in TBST to detect total $GABA_BRs$ and the other group was not permeabilized to detect only surface expression. The slices were blocked and incubated with the following primary antibodies that recognize only the N-terminus (extracellular) domain of $GABA_BR1$ (mouse anti-$GABA_BR1$, Cat# ab55051, RRID: AB_941703, 1:500) or the N-terminus (extracellular) domain of $GABA_BR2$ (Rabbit anti-$GABA_BR2$, Cat# 4819, RRID: AB_2108339, 1:750) for 24 h at room temperature. The slices were then washed and incubated with appropriate secondary fluorescent antibodies for 30 min. After repetitive washings with TBS, the slices were mounted with sRIMS buffer and mean fluorescence intensity was measured from layers II/III somatosensory cortices with the Visiscope spinning-disc confocal system.

Western blotting

Equal amounts of cortical tissue samples (22.5 µg) were homogenized in urea assay lysis buffer (100 mM Tris-HCl, pH= 7.5; 12 mM magnesium acetate tetrahydrate and 6M urea) with protease and phosphatase inhibitors and then centrifuged at 14,000 rpm for 15 min to remove debris and nuclei. The SDS loading buffer was run on a 10% SDS-polyacrylamide gel and transferred to a nitrocellulose membrane for 1 h 40 min in transfer buffer (25 mM Tris/Base, 192 mM glycine). Membranes were then blocked for 1 h at room temperature

(RT) while shaking in blocking buffer with TBS (Cat# P/N 927-50000, Li-Cor, Bad Homburg, Germany). Membranes were incubated overnight (O/N) at 4 °C with the primary antibody and for 2h at RT with the secondary antibody. After each incubation step, membranes were washed for 3 × 15 min in TBS with 0.1% Tween 20. Membranes were imaged with the Odyssey immunoblot software (Lincoln). The Odyssey software system was also used for densitometric analysis. The following antibodies were used: Rabbit anti-$GABA_BR2$ (Cat# 4819, RRID: AB_2108339, 1:500) , mouse anti-$GABA_BR1$ (Cat# ab55051, Abcam, Cambridge, UK, 1:500), rabbit anti-$GABA_BR2$ p-Ser 783 (Cat# TA309142, OriGene Technologies, Herford, Germany, 1:1000), p-$GABA_BR2$ S892 (Cat# PPS073, RRID: AB_2108325, 1:1000), mouse anti-Reelin G10 ((Cat# MAB5364, RRID: AB_2179313, 1:1000), and ß-Actin (Cat# ab8227, RRID:AB_2305186,1:10000).

Statistical analysis

Statistical analysis was performed with Sigma Stat 12 (SPSS Incorporated). The data are presented as box plots with median (center line), minimum, and maximum (whiskers), and 25th–75th percentiles (box). Comparisons between two groups were performed with Students unpaired T-test when normality test (Shapiro-Wilk) passed, otherwise the Mann–Whitney test. Comparisons between groups larger than two were performed with one-way-ANOVA and a Holm-Sidak Multiple Comparison Test for post-hoc analysis if normality test passed. If normality failed, we run One-Way-Anova on Ranks followed by Tukey's multiple comparison test for post hoc analysis to isolate the significant groups. If the sample sizes were unequal, the Dunn`s multiple comparison test was used to isolate the significant groups. Results were considered statistically significant at $p<0.05$.

Results

Cortical layering is not altered after postnatal loss of Reelin in $Reln^{cKO}$ mice

To bypass the cortical layer malformations that are present in the reeler mutant, tamoxifen was fed to newborn pups (~P1) for 5 consecutive days. Around P14, animals were sacrificed, and sections of cortical tissue were subjected to immunohistochemical staining (Fig. S1). First, we confirmed that tamoxifen administration induces nuclear Cre activation and knockout of the floxed Reelin gene. We found that tamoxifen administration at P1 induced complete elimination of Reelin immunostaining at P14 (Fig. S1A). The pattern of immunostaining against wolframin (Wfs1), a protein expressed by layer II and IV neurons in the mouse somatosensory cortex, was indistinguishable from wt (Fig. S1B), while the layer-specific distribution of this protein is disrupted in the reeler cortex (Boyle et al. 2011). Next, we examined the distribution of cut-like homeobox 1 (Cux-1) protein, a transcription factor expressed in neurons throughout layers II–IV. In the cortex of adult reeler mice, most Cux-1-positive neurons are found in cortical layers V and VI and do not respect the strict boundary that characterizes wildtype cortical layering (Nieto et al. 2004). The distribution of Cux-1 immunostaining in the cortex of $Reln^{cKO}$ mice was found in the supragranular layers II-IV and was indistinguishable from wt (Fig. S1C). We then examined the distribution of the fast-spiking interneuron marker Parvalbumin (Parv) and found it to be unchanged in the $Reln^{cKO}$ when compared to wildtype mice (Fig. S1D). These findings confirm that postnatal Reelin

elimination did not alter the distribution of layer specific expression markers in the neocortex.

Excessive Ca^{2+} spike frequency in early postnatally Reelin-deficient $Reln^{cKO}$ mice

Using Ca^{2+} imaging, we compared spontaneous activity in acute slices prepared from wt and $Reln^{cKO}$ littermates at P14 (both pup groups were fed with tamoxifen). In our experience (Hamad et al. 2015) as well as in other studies (Yuste et al. 2011), imaging a large network of neuronal populations loaded with the calcium indicator OGB-1 AM under a spinning-disk confocal microscope, equipped with fast cameras, can be used to image thousands of neurons simultaneously without significant photobleaching, with good signal-to-noise ratio and minimized cellular damage because it does not require electrodes penetrating the tissue. To ensure that tamoxifen *per se* did not alter basic synaptic transmission, we recorded Ca^{2+} amplitude and frequency in DIV14 (days in vitro 14) OTCs loaded with OGB-1 AM from wt mice which were stimulated for 5 consecutive days either with 4-hydroxytamoxifen (4-OHT) or vehicle (DMSO) as a control group (Fig. S2). Neither 4-OHT nor vehicle groups showed any difference in Ca^{2+} amplitude, frequency or Ca^{2+} transient half-width when compared to the untreated wt control group (Fig. S2). Next, we compared Ca^{2+} signal amplitude, frequency and Ca^{2+} transient half-width in wt and $Reln^{cKO}$ slices using the Ca^{2+} indicator OGB-1 AM (Fig. 1B-F). Ca^{2+} amplitudes were not altered in $Reln^{cKO}$ when compared to the wt control group (Fig. 1D). Strikingly, the Ca^{2+} frequency and Ca^{2+} transient half-width were significantly increased in $Reln^{cKO}$ (Fig. 1E and F). Recordings were performed in acute slices prepared at P14 and transfected with a genetic construct encoding the Ca^{2+} indicator GCaMP6s (Chen et al. 2013). GCaMP6s is very sensitive to Ca^{2+} changes and we found it to be distributed in soma, dendrites and axon (Fig. 1G). Criteria to distinguish pyramidal cells and interneurons were based on dendritic and axonal patterns (Hamad et al. 2011; Hamad et al. 2014; Karube et al. 2004; Kawaguchi et al. 2006). To confirm the cell type, after Ca^{2+} recording, acute slices were fixed and stained against glutamate decarboxylase-65 (GAD-65) which labels the GABA biosynthesis enzyme in the soma of all GABAergic interneurons but does not label glutamatergic pyramidal cells (Fig. S3). Our results confirmed an unchanged amplitude in $Reln^{wt}$ compared to $Reln^{cKO}$ in both pyramidal cells and interneurons (Fig. 1H) and revealed an enhanced frequency and Ca^{2+} transient half-width in both pyramidal cells and interneurons in the $Reln^{cKO}$ (Fig. 1I and J), suggesting that $Reln^{cKO}$ mice exhibit defects at the presynaptic level. Moreover, Ca^{2+} amplitude and Ca^{2+} transient half-width did not differ between pyramidal cells and interneurons in both wt and $Reln^{cKO}$ slices during GCaMP6s recordings, confirming a previously published study (Weir et al. 2014). Therefore, the subsequent recording experiments were performed with the calcium dye OGB-1 AM.

Wildtype Reelin rescues Ca^{2+} frequency in $Reln^{cKO}$ neurons

Next, we investigated whether secreted Reelin from wt OTCs might rescue the abnormal neuronal activity observed in the $Reln^{cKO}$ OTCs. To address this question, we co-cultured OTCs as follows: wt + wt, or $Reln^{cKO}$ + $Reln^{cKO}$, or wt + $Reln^{cKO}$ (Fig. 2B). To detect the abundance of secreted Reelin in the culture medium under these three conditions, we quantified secreted Reelin protein with western blot from culture medium. As expected, the amount of secreted Reelin was abundant in the wt + wt, a lesser amount was detectable in

the wt + Reln^{cKO}, whereas Reelin was almost undetectable in the Reln^{cKO} + Reln^{cKO} co-culture medium (Fig. 2C and D). Ca^{2+} recordings experiments showed that the Ca^{2+} amplitude did not change under any of the three experimental conditions (Fig. 2E) confirming our interpretation that Reelin does not affect postsynaptic activity. However, in the Reln^{cKO} OTCs co-cultured with wt, the Ca^{2+} frequency and Ca^{2+} transient half-width in the recorded Reln^{cKO} OTC was reduced to the same level as in the wt OTC (Fig. 2F and G). These results suggest that Reelin secreted from wt OTCs into the incubation medium restored presynaptic activity in Reln^{cKO} OTCs to a basic level comparable to the wt control group.

GABA$_B$R function is impaired in Reln^{cKO} mice

GABA$_B$Rs are present in GABAergic neuronal terminals (as autoreceptors) and in glutamatergic and other terminals (heteroreceptors) (Benarroch 2012). Around the second postnatal week, the only source of Reelin in the neocortex are inhibitory interneurons (Pohlkamp et al. 2014). We speculated that the increased Ca^{2+} spiking frequency in Reln^{cKO} mice in pyramidal cells and interneurons that we observed, was likely due to a defect of GABA$_B$R function at the GABAergic or glutamatergic presynaptic terminal. If presynaptic GABA$_B$Rs at the GABAergic neuronal terminals were defective in Reln^{cKO} mice, activated GABA$_B$Rs would no longer be able to block Ca^{2+} channels because presynaptic GABA$_B$ receptors inhibit N type (Cav2.2) or P/Q type ($Ca_v2.1$) Ca^{2+} channels, resulting in reduced neurotransmitter release (Benarroch 2012). In turn, Ca^{2+} channels trigger the release of GABA, and thereby inhibit neighbouring cells. However, Reln^{cKO} mice exhibited a higher Ca^{2+} frequency when compared to wt control (Fig. 1), suggesting that presynaptic GABA$_B$Rs at GABAergic neuronal terminals were not defective in Reln^{cKO} mice. Therefore, we tested a second possibility, i.e. defective presynaptic GABA$_B$Rs at glutamatergic terminals in Reln^{cKO} mice. To test this possibility, we recorded wt and Reln^{cKO} OTCs in the presence of the AMPA- and kainate receptor blocker CNQX and the NMDARs antagonist APV at DIV14 (Fig. S4). Bath application of 10 μM CNQX immediately decreased the Ca^{2+} amplitude, frequency and Ca^{2+} transient half-width in Reln^{cKO} to the same extent as in the wt control group (Fig. S4 A and B). Similarly, APV application elicited the same effect (Fig. S4 D-F). The observation that the excessive Ca^{2+} frequency in the Reln^{cKO} can be blocked with CNQX or APV suggests that glutamatergic signaling in the absence of Reelin is still functional. Taken together, we conclude from our findings that most likely GABA$_B$Rs at glutamatergic presynaptic terminals are defective in the Reln^{cKO}. Moreover, We preclude a possible defect of GABA$_B$Rs at the postsynaptic site because no significant change in the Ca^{2+} amplitude was observed (Fig. 1).

To examine a possible crosstalk between Reelin signaling and GABA$_B$R function, we prepared OTCs from P0 mice. OTCs were treated with 4-OHT at DIV1-5 to induce Reelin deficiency. Subsequent Reelin knockout, Ca^{2+}-recordings were performed around DIV14 (Fig. 3). First, to confirm conditionally induced Reelin knockout, OTCs were fixed at DIV14 and immunostained against Cre-recombinase and Reelin (Fig. S5). While pronounced Reelin staining was seen in wt OTCs, it was absent in Reln^{cko} OTCs. Bath application of the GABA$_B$R agonist baclofen (10 μM) immediately activated GABA$_B$Rs and strongly decreased the Ca^{2+} amplitude by 6-fold in wt OTCs, but to a lesser extent (1.6-fold) in

Reln^{cKO} OTCs (Fig. 3A), suggesting that postsynaptic GABA$_B$Rs were still functioning in Reln^{cKO} OTCs. However, we do not preclude a postsynaptic functional difference between wt and Reln^{cKO}. Moreover, baclofen induced a profound reduction of the Ca^{2+} frequency and Ca^{2+} transient half-width in wt OTCs (Fig. 3B and C and Movie S1), but no effect was observed in Reln^{cKO} OTCs (Fig. 3B, C and Movie S2). This suggests an altered GABA$_B$R function at presynaptic sites in Reln^{cKO}, probably due to a lack of trafficking and localization of GABA$_B$Rs at the plasma membrane in Reln^{cKO} mice. Strikingly, the GABA$_B$R antagonist CGP35348 (10 μM) did not influence the Ca^{2+} amplitude, neither in wt nor in Reln^{cKO} OTCs (Fig. 3D). However, blockade of GABA$_B$Rs in wt OTCs dramatically increased the Ca^{2+} signaling frequency and Ca^{2+} transient half-width in wt but not in Reln^{cKO} OTCs (Fig. 3E and F). Taken together, these results indicate a presynaptic dysfunction of GABA$_B$Rs in the Reln^{cKO} OTCs.

Presynaptic GABA$_B$Rs are modulated by Reelin signaling

Based on our observation that presynaptic GABA$_B$Rs do not properly function in the absence of Reelin, we wondered whether the function of GABA$_B$Rs might be modulated by canonical Reelin signaling. To address this question, we treated OTCs with RAP, an inhibitor of low-density lipoprotein receptor–related proteins (including VLDL and APOER2; (Herz et al. 1991; Willnow et al. 1996)). Reelin acts via binding to VLDLR and ApoER2 to regulate Dab1 tyrosine phosphorylation (Cooper and Howell 1999; Trommsdorff et al. 1999). We have found that chronic RAP treatment (50 ng/ml, over 5 days) did not affect the Ca^{2+} amplitude in Reln^{cKO} and wt OTCs (Fig. 4A). However, RAP blockade in wt OTCs enhanced the Ca^{2+} frequency and Ca^{2+} transient half-width to a comparable extent as seen in the Reln^{cKO} without RAP treatment (Fig. 4B and C). As expected, Reln^{cKO} OTCs treated with RAP did not exhibit any changes in frequency and Ca^{2+} transient half-width (Fig. 4B and C). These observations suggest that GABA$_B$Rs require crosstalk with Reelin signaling for their proper function.

Reelin activates members of Src family tyrosine kinases (SFKs) via ApoER2 and VLDLR and Dab1 (Bock and Herz 2003; Cooper and Howell 1999). Therefore, we addressed the question whether inhibition of Src family kinases with the pharmacological blocker PP2 might affect GABA$_B$R function. Our results show that the application of 1 μM PP2 at DIV14 did not alter the Ca^{2+} amplitude neither in wt nor in Reln^{cKO} OTCs (Fig. 5A). In turn, the Ca^{2+} frequency and Ca^{2+} transient half-width were increased in wt only but not Reln^{cKO} OTCs (Fig. 5B and C). To test whether the inhibition of Src family kinases with the pharmacological blocker PP2 might also affect GABA$_B$R surface expression, OTCs from wt and Reln^{cKO} mice were treated with 1 μM PP2 and immunostained against GABA$_B$R1 and GABA$_B$R2 under non-permeabilized condition to detect their surface expression (Fig. S6). The surface expression of GABA$_B$R1 and GABA$_B$R2 was significantly reduced in wt OTC but remained unaltered in the Reln^{cKO}. Together, these results suggest that Reelin signaling through Src is important to maintain GABA$_B$Rs function and surface expression. In line with these findings, a previous study had shown that the expression of SNAP25, a protein that is involved in the control of transmitter release, was decreased in the hippocampus of reeler mutant mice, but not altered in ApoER2-, VLDLR-, or Dab1-deficient mice (Hellwig et al. 2011). Moreover, GABA$_B$Rs were found to be downregulated in the reeler mutant (Cremer

et al. 2011). Taken together, our findings suggest that presynaptic $GABA_BR$ function is modulated through the Reelin signaling cascade.

Reelin signaling alters $GABA_BR2$ cell surface expression and its phosphorylation at S783 and S892

Previous studies have demonstrated that $GABA_BRs$ do not undergo agonist-induced internalization (Terunuma, Pangalos et al. 2010), and that $GABA_BR$ cytoplasmic domains contain multiple phosphorylation sites (Couve et al. 2002; Fairfax et al. 2004). To find out whether Reelin deficiency might affect $GABA_BR$ cell surface expression, we performed immunofluorescence staining of $GABA_BR1$ and $GABA_BR2$ with specific antibodies that recognize only the extracellular N-terminal domain of the receptor subunits (Fig. 6). Mean fluorescence intensity analysis revealed that both $GABA_BR1$ and $GABA_BR2$ surface staining was significantly reduced in non-permeabilized cells of $Reln^{cKO}$ acute slices in comparison to wt (Fig. 6), suggesting a role of Reelin in regulating $GABA_BR$ cell surface expression. Next, we investigated whether secreted Reelin from wt OTCs might rescue the reduction of $GABA_BR1$ and $GABA_BR2$ surface expression in the $Reln^{cKO}$. To address this question, we co-cultured OTCs from wt + $Reln^{cKO}$ (Fig. S7). Our results show that Reelin secreted from wt OTCs into the incubation medium maintained $GABA_BR1$ and $GABA_BR2$ expression in $Reln^{cKO}$ at a level comparable to the wt control group.

Finally, we performed western blotting, to assess the amount of expressed $GABA_BR1$ and $GABA_BR2$ protein, which however, did not differ significantly between wt and $Reln^{cKO}$, though the amount of both receptors showed a tendency to decrease in the $Reln^{cKO}$ (Fig. 7A and B). To find out whether Reelin deficiency might affect $GABA_BR$ phosphorylation, we analysed cortical lysates from wt and $Reln^{cKO}$ P14 mice by western blotting with antibodies against $GABA_BR$ phosphorylation sites. $GABA_BR2$ phosphorylation at Ser892 is mediated by cyclic AMP (cAMP)–dependent protein kinase (PKA) and stabilizes cell surface expression and coupling to G-proteins of the receptors (Couve et al. 2002). Western blotting revealed that in Reelin deficient tissue, S892 phosphorylation of $GABA_BR2$ was significantly reduced when compared to wt (Fig. 7C), suggesting that Reelin signaling is important to stabilize $GABA_BR2$ function at the cell surface. Another $GABA_BR2$ phosphorylation site at S783 is required for degradation, and its phosphorylation is mediated by 5′-AMP-dependent protein kinase (AMPK) (Terunuma, Vargas et al. 2010). $GABA_BR2$ recycling and degradation is controlled via phosphorylation site S783 (Gassmann and Bettler 2012). Western blot analysis revealed that $GABA_BR2$ phosphorylation at S783 in $Reln^{cKO}$ mice was in creased when compared to wt, and that phosphorylated $GABA_BR2s$ were degraded in $Reln^{cKO}$ mice only (Fig. 7D). Taken together, these findings indicate that Reelin is required to stabilize the cell surface expression of functional $GABA_BR2$ receptors, probably by inhibiting receptor degradation.

$GABA_BR$ intracellular signaling via $G\alpha i/o$ proteins is affected in $Reln^{cKO}$ mice

To further investigate a potential crosstalk between Reelin, $GABA_BR$ signaling and G-protein coupled receptors, we recorded OTCs in the presence of pertussis toxin (PTX). Stimulation of $GABA_BRs$ with baclofen inhibits adenylyl cyclase (Xu and Wojcik 1986), which in turn can be blocked by pertussis toxin (PTX), known to inhibit G-protein function

(Karbon and Enna 1985; Nishikawa and Kuriyama 1989). Application of PTX at DIV14 enhanced the Ca^{2+} amplitude, frequency and Ca^{2+} transient half-width in wt but not in $Reln^{cKO}$ OTCs (Fig. S8). These results further support the interpretation that Ca^{2+}-signalling is unaltered by the treatment in $Reln^{cKO}$ OTCs because $GABA_BR$ receptors are degraded in the absence of Reelin. It also confirms that Reelin is important to maintain proper $GABA_BR$ signaling.

Discussion

In the present study, we characterized a novel role of Reelin in early postnatal cortical function. We found that postnatally induced Reelin deficiency caused abnormal Ca^{2+} spike frequency and Ca^{2+} transient half-width in cortical neurons. RAP blockade of Reelin binding to its receptors ApoER2 and VLDLR mimicked this effect. There are no specific selective antagonists for ApoER2 and VLDLR, therefore we used RAP to broadly block LRP family members. Co-culture of $Reln^{cKO}$ OTCs with Reelin secreting wt OTCs rescued deficient network activity in $Reln^{cKO}$ OTCs. While the $GABA_BR$ agonist baclofen failed to activate $GABA_BRs$, the $GABA_BR$ antagonist CGP35348 failed to inhibit $GABA_BRs$ in $Reln^{cKO}$ OTCs, indicating deactivation and/or degradation of $GABA_BRs$ in $Reln^{cKO}$ OTCs. Immunostaining of non-permeabilized cells with antibodies against $GABA_BR1$ and $GABA_BR2$ extracellular domains was significantly reduced in $Reln^{cKO}$ slices in line with our pharmacological experiments, and confirming a previous study that reported on a downregulation of $GABA_BRs$ in the reeler mutant (Cremer et al. 2011). When analysing cortical tissue of conditionally induced Reelin deficient mice by western blotting, we found a decreased $GABA_BR2$ phosphorylation at S892 and an increased phosphorylation at S783, both indicative of $GABA_BR2$ degradation (Gassmann and Bettler 2012), and proteolytic processing of $GABA_BR2$. Accordingly, in $Reln^{cKO}$ slices we observed a decrease in surface expression of $GABA_BR1$ (approx. 35% decrease) and $GABA_BR2$ (approx. 39% decrease) respectively. The enhanced Ca^{+2} frequency in the $Reln^{cKO}$ slices can be attributed to the degradation (downregulation) of the $GABA_BRs$ at the presynaptic sites. The main function of presynaptic $GABA_BRs$ at the presynaptic site is to inhibit calcium channels, which results in inhibition of neurotransmitter release (Benarroch 2012). Together, our findings suggest a novel role for Reelin in controlling cortical neuronal network maturation, by regulating Ca^{2+} spiking in glutamatergic neurons via presynaptic $GABA_BRs$.

Prolonged NMDA-R stimulation triggered both the endocytosis of $GABA_BRs$ (Terunuma, Vargas et al. 2010) and activation of PP2A. PP2A in turn favors dephosphorylation of S783 in GABABR2 and redirection of the endocytosed pool from recycling to degradation. However, Surprisingly, despite the observed dephosphorylation of S783 in GABAergic neurons, no increase in the lysosomal degradation of $GABA_BRs$ has been observed by (Padgett et al. 2012). The identification of S783 on the $GABA_BR2$ subunit as an AMPK substrate points to a link between the induction of ischemia and increased phosphorylation of $GABA_BRs$ in the hippocampus (Kuramoto et al. 2007). The increase in GABAB receptor phosphorylation, evident during ischemia, could provide a potentially neuroprotective mechanism that may limit neuronal exposure to excitotoxicity. In absence of Reelin, we also observed enhanced Ca2+ signalling in the $Reln^{cKO}$ and increased phosphorylation at Ser783, which might similarly be important to protect neurons from excitotoxicity.

By performing immunohistochemical staining with antibodies against layer-specific markers, we confirm that cortical neurons in postnatal $Reln^{cKO}$ did not alter their characteristic layer specific marker expression in the absence of Reelin (Boyle et al. 2011). There are two populations of Reelin expressing neurons in the neocortex. At early embryonic stages, Reelin is secreted by Cajal-Retzius (CR) cells. The number of CR cells declines postnatally, and these cells disappear almost completely around P14 by undergoing selective cell death through apoptosis (Anstötz et al. 2014). Moreover, almost all GABAergic interneurons in the neonatal cortex express Reelin, suggesting that in the current study Reelin was mainly expressed by interneurons.

A role of Reelin in modulating glutamatergic activity has been previously reported (Chen et al. 2005). Reelin-haploinsufficiency has been shown to disrupt the developmental course of GABA excitatory/inhibitory balance (Bouamrane et al. 2016). In the current experiments, we studied spontaneous neuronal calcium activity in the $Reln^{cKO}$ compared to wt littermates. While the Ca^{2+} amplitude was unaltered in RelncKO, the frequency of Ca^{2+} spiking and Ca^{2+} transient half-width was dramatically increased in $Reln^{cKO}$ when compared to wt. The Ca^{2+} spike half-width narrows around the second postnatal week (14DIV or P14) and this observation has been previously attributed to an increase in cell size and maturation of ion channels (Gold et al. 2007). Thus, the increased Ca^{2+} spikes half-width in $Reln^{cKO}$ may suggest an immature ion channels condition in these mice. Along this line, related observations were reported in the reeler hippocampus. Thus, using electron microscopy, it has been shown that the number of presynaptic vesicles was significantly increased in hippocampal CA1 synapses of reeler mutant mice when compared to wt (Hellwig et al. 2011). In contrast, acute Reelin application to dissociated hippocampal neurons enhanced spontaneous neurotransmitter release without affecting properties of evoked neurotransmission (Bal et al. 2013). The discrepancy here may be due to the different models and methodologies used. For instance, acute application of 5 nM Reelin (Bal et al. 2013) versus analysis of the reeler mutant (Hellwig et al. 2011) or the $Reln^{cKO}$ (present study). In neocortical neurons, neurotransmitter release is controlled by $GABA_BR$ function (see Introduction). Moreover, perturbations of GABAB receptor signaling during development may shift the excitatory/inhibitory balance, culminating in various neurological dysfunctions, including typical and atypical absence seizures (Han et al. 2012). To find out whether Reelin function might interfere with $GABA_BR$ function, we manipulated $GABA_BR$ physiology in $Reln^{cKO}$ tissue using pharmacological agents. Our observation that a $GABA_BR$ agonist failed to activate $GABA_BRs$ and an antagonist failed to inhibit $GABA_BRs$ in the $Reln^{cKO}$, points to a novel function of Reelin as a modulator of $GABA_BRs$ during early cortical function. Taken together, our data suggest that in the absence of Reelin, $GABA_BRs$ are downregulated, as shown by $GABA_BR$ cell surface immunolabelling experiments, and by western blotting that revealed an altered $GABA_BR$ phosphorylation status as well as proteolytic receptor processing.

Next, we investigated possible mechanisms underlying cross-talk of Reelin and $GABA_BR$ signaling. Binding of Reelin to its receptors induces phosphorylation of Dab1 protein by Src kinase (Bock and Herz 2003). Blocking of wt OTCs with a Src inhibitor increased the Ca^{2+} signaling frequency to a comparable level as in $Reln^{cKO}$. Moreover, the Src inhibitor decreased $GABA_BRs$ surface expression in wt slices but it did not affect $GABA_BRs$ surface

expression in the $Reln^{cKO}$. These observations suggest that Reelin signaling through Src is important to maintain $GABA_BRs$ function. Src may directly interact with the α subunits of G-proteins (Ma et al. 2000) and recently it has been shown that Src/Gαo interactions provide evidence for a novel type of cross-talk between a non-receptor tyrosine kinase stimulated by Reelin and heterologous G protein-coupled receptors (GPCR) (Cho et al. 2015). Since $GABA_BRs$, are members of the G-protein coupled receptors (GPCRs), it is very well possible that metabotropic $GABA_BRs$ are modulated by Reelin through Src-kinase.

Stimulation of $GABA_BRs$ with baclofen can inhibit both basal, and forskolin stimulated adenylyl cyclase (Xu and Wojcik 1986), which in turn can be blocked by pertussis toxin (PTX), reflecting the involvement of the Giα- and Goα- subunit of the G-protein (Karbon and Enna 1985; Nishikawa and Kuriyama 1989). Moreover, immunoprecipitation assays disclosed the possibility that Reelin might increase the active forms of both Src and Gαo and promote their direct association (Cho et al. 2015). Thus, our finding that PTX increases Ca^{2+} frequency in wt OTCs but not in $Reln^{cKO}$, indicates the possibility of a disrupted Src-Gαi/o interaction in the absence of Reelin. For instance, based on our experiments it appears more likely that reduced cell surface expression of $GABA_BR$ is the reason why Ca^{2+} signalling is unaltered in $Reln^{cKO}$ OTCs after PTX application.

Functional deficits associated with decreased Reelin expression have often been attributed to the well-known developmental neuronal migration defects in Reelin deficient mice (Eastwood and Harrison 2003). Moreover, both Reelin deficiency and cortical network dysrhythmias caused by aberrant interneuron activity were also discussed as possible factors contributing to cognitive and behavioural deficits in Alzheimer disease (AD) (Palop and Mucke 2016; Xiao et al. 2017). Besides Reelin, also different ApoE isoforms act as lipoprotein receptor ligands and are known to influence AD pathogenesis, with ApoE4 being the most important genetic risk factor for AD (Huang et al. 2017). $GABA_BRs$ were repeatedly shown to be implicated in synaptic plasticity (Davies et al. 1991; Mott and Lewis 1991). Until recently, it remained unclear whether $GABA_BRs$ can influence neuronal plasticity through $GABA_BRs$ signaling. It has been demonstrated that G-protein mediated signaling through $GABA_BRs$ delays the recruitment of synaptic vesicles during sustained activity and after short-term depression (Sakaba and Neher 2003). This delay occurs through a reduction of cAMP, which in turn blocks the stimulatory effect of the increased Ca^{2+} concentration on vesicle recruitment (Sakaba and Neher 2003). In conclusion, we provide evidence for a novel role of Reelin signaling in controlling early neuronal network activity by regulating neurotransmitter release through $GABA_BRs$.

Supplementary Material

Refer to Web version on PubMed Central for supplementary material.

Acknowledgments

Funding: This work was supported by the National Institutes of Health grant R37 HL63762, R01 NS093382, R01 NS108115, and RF1 AG053391, the Consortium for Frontotemporal Dementia Research; the Bright Focus

Foundation and a Harrington Innovator Award to J. H., E. F. was supported by FoRUM of the Ruhr-Universität Bochum.

Abbreviations:

ACSF	artificial cerebrospinal fluid
ANOVA	Analysis of variance
APV	(2R)-amino-5-phosphonopentanoate
CNQX	6-cyano-7-nitroquinoxaline-2,3-dione
Cux-1	cut-like homeobox 1
DIV	Days in vitro
DAB1	Disabled-1
F^0	baseline fluorescence
GAD65	Glutamate Decarboxylase-65
GABA	gamma-aminobutyric acid
LRPAP Protein = RAP	LDL receptor-related protein-associated protein 1
OGB-1 AM	Oregon Green BAPTA-1 Acetoxymethyl
OTCs	Organotypic cultures
4-OHT	(Z)-4-hydroxytamoxifen
PFA	paraformaldehyde
P	postnatal day
Parv	Parvalbumin
PTX	pertussis toxin
$Reln^{cKO}$	Reelin conditional knock-out mice
ROI	region of interest
RRID	research resource identifier
TBS	Tris buffered Saline
WFS	Wolframin 1
WT	$Reln^{flox/flox}$ wildtype

References

Anstötz M, Cosgrove KE, Hack I, Mugnaini E, Maccaferri G and Lübke JHR (2014) Morphology, input-output relations and synaptic connectivity of Cajal-Retzius cells in layer 1 of the developing neocortex of CXCR4-EGFP mice. Brain Struct Funct 219, 2119–2139. [PubMed: 24026287]

Bal M, Leitz J, Reese AL, Ramirez DMO, Durakoglugil M, Herz J, Monteggia LM and Kavalali ET (2013) Reelin mobilizes a VAMP7-dependent synaptic vesicle pool and selectively augments spontaneous neurotransmission. Neuron 80, 934–946. [PubMed: 24210904]

Ben-Ari Y, Gaiarsa J-L, Tyzio R and Khazipov R (2007) GABA. Physiol Rev 87, 1215–1284. [PubMed: 17928584]

Ben-Ari Y, Woodin MA, Sernagor E, Cancedda L, Vinay L, Rivera C, Legendre P, Luhmann HJ, Bordey A, Wenner P, Fukuda A, van den Pol AN, Gaiarsa J-L and Cherubini E (2012) Refuting the challenges of the developmental shift of polarity of GABA actions. Front Cell Neurosci 6, 35. [PubMed: 22973192]

Benarroch EE (2012) GABAB receptors. Neurology 78, 578–584. [PubMed: 22351795]

Bettler B, Kaupmann K, Mosbacher J and Gassmann M (2004) Molecular structure and physiological functions of GABA(B) receptors. Physiol Rev 84, 835–867. [PubMed: 15269338]

Bock HH and Herz J (2003) Reelin activates SRC family tyrosine kinases in neurons. Curr Biol 13, 18–26. [PubMed: 12526740]

Bock HH and May P (2016) Canonical and Non-canonical Reelin Signaling. Front Cell Neurosci 10, 166. [PubMed: 27445693]

Bouamrane L, Scheyer AF, Lassalle O, Iafrati J, Thomazeau A and Chavis P (2016) Reelin-Haploinsufficiency Disrupts the Developmental Trajectory of the E/I Balance in the Prefrontal Cortex. Front Cell Neurosci 10, 308. [PubMed: 28127276]

Boyle MP, Bernard A, Thompson CL, Ng L, Boe A, Mortrud M, Hawrylycz MJ, Jones AR, Hevner RF and Lein ES (2011) Cell-type-specific consequences of Reelin deficiency in the mouse neocortex, hippocampus, and amygdala. J Comp Neurol 519, 2061–2089. [PubMed: 21491433]

Bu G and Schwartz AL (1998) RAP, a novel type of ER chaperone. Trends Cell Biol 8, 272–276. [PubMed: 9714598]

Caviness VS (1976) Patterns of cell and fiber distribution in the neocortex of the reeler mutant mouse. J Comp Neurol 170, 435–447. [PubMed: 1002868]

Caviness VS (1982) Neocortical histogenesis in normal and reeler mice. Brain Res 256, 293–302. [PubMed: 7104762]

Caviness VS and Sidman RL (1973) Time of origin or corresponding cell classes in the cerebral cortex of normal and reeler mutant mice. J Comp Neurol 148, 141–151. [PubMed: 4700506]

Chen T-W, Wardill TJ, Sun Y, Pulver SR, Renninger SL, Baohan A, Schreiter ER, Kerr RA, Orger MB, Jayaraman V, Looger LL, Svoboda K and Kim DS (2013) Ultrasensitive fluorescent proteins for imaging neuronal activity. Nature 499, 295–300. [PubMed: 23868258]

Chen Y, Beffert U, Ertunc M, Tang T-S, Kavalali ET, Bezprozvanny I and Herz J (2005) Reelin modulates NMDA receptor activity in cortical neurons. J Neurosci 25, 8209–8216. [PubMed: 16148228]

Cho S-K, Choi J-M, Kim J-M, Cho JY, Kim S-S, Hong S, Suh-Kim H and Lee Y-D (2015) AKT-independent Reelin signaling requires interactions of heterotrimeric Go and Src. Biochem Biophys Res Commun 467, 1063–1069. [PubMed: 26441085]

Cooper JA and Howell BW (1999) Lipoprotein receptors. Cell 97, 671–674. [PubMed: 10380917]

Couve A, Thomas P, Calver AR, Hirst WD, Pangalos MN, Walsh FS, Smart TG and Moss SJ (2002) Cyclic AMP-dependent protein kinase phosphorylation facilitates GABA(B) receptor-effector coupling. Nat Neurosci 5, 415–424. [PubMed: 11976702]

Cremer CM, Lübke JHR, Palomero-Gallagher N and Zilles K (2011) Laminar distribution of neurotransmitter receptors in different reeler mouse brain regions. Brain Struct Funct 216, 201–218. [PubMed: 21442415]

Curran T and D'Arcangelo G (1998) Role of reelin in the control of brain development. Brain Res Brain Res Rev 26, 285–294. [PubMed: 9651544]

D'Arcangelo G, Homayouni R, Keshvara L, Rice DS, Sheldon M and Curran T (1999) Reelin is a ligand for lipoprotein receptors. Neuron 24, 471–479. [PubMed: 10571240]

Davies CH, Starkey SJ, Pozza MF and Collingridge GL (1991) GABA autoreceptors regulate the induction of LTP. Nature 349, 609–611. [PubMed: 1847993]

Dazzo E, Fanciulli M, Serioli E, Minervini G, Pulitano P, Binelli S, Di Bonaventura C, Luisi C, Pasini E, Striano S, Striano P, Coppola G, Chiavegato A, Radovic S, Spadotto A, Uzzau S, La Neve A, Giallonardo AT, Mecarelli O, Tosatto SCE, Ottman R, Michelucci R and Nobile C (2015) Heterozygous reelin mutations cause autosomal-dominant lateral temporal epilepsy. Am J Hum Genet 96, 992–1000. [PubMed: 26046367]

Eastwood SL and Harrison PJ (2003) Interstitial white matter neurons express less reelin and are abnormally distributed in schizophrenia. Mol Psychiatry 8, 769, 821–31.

Fairfax BP, Pitcher JA, Scott MGH, Calver AR, Pangalos MN, Moss SJ and Couve A (2004) Phosphorylation and chronic agonist treatment atypically modulate GABAB receptor cell surface stability. J Biol Chem 279, 12565–12573. [PubMed: 14707142]

Fukuda A, Mody I and Prince DA (1993) Differential ontogenesis of presynaptic and postsynaptic GABAB inhibition in rat somatosensory cortex. J Neurophysiol 70, 448–452. [PubMed: 8395587]

Gassmann M and Bettler B (2012) Regulation of neuronal GABA(B) receptor functions by subunit composition. Nat Rev Neurosci 13, 380–394. [PubMed: 22595784]

Gold C, Henze DA and Koch C (2007) Using extracellular action potential recordings to constrain compartmental models. J Comput Neurosci 23, 39–58. [PubMed: 17273940]

Gong C, Wang T-W, Huang HS and Parent JM (2007) Reelin regulates neuronal progenitor migration in intact and epileptic hippocampus. J Neurosci 27, 1803–1811. [PubMed: 17314278]

Guy J, Wagener RJ, Möck M and Staiger JF (2015) Persistence of Functional Sensory Maps in the Absence of Cortical Layers in the Somsatosensory Cortex of Reeler Mice. Cereb Cortex 25, 2517–2528. [PubMed: 24759695]

Hamad MIK, Jack A, Klatt O, Lorkowski M, Strasdeit T, Kott S, Sager C, Hollmann M and Wahle P (2014) Type I TARPs promote dendritic growth of early postnatal neocortical pyramidal cells in organotypic cultures. Development 141, 1737–1748. [PubMed: 24667327]

Hamad MIK, Krause M and Wahle P (2015) Improving AM ester calcium dye loading efficiency. J Neurosci Methods 240, 48–60. [PubMed: 25448382]

Hamad MIK, Ma-Högemeier Z-L, Riedel C, Conrads C, Veitinger T, Habijan T, Schulz J-N, Krause M, Wirth MJ, Hollmann M and Wahle P (2011) Cell class-specific regulation of neocortical dendrite and spine growth by AMPA receptor splice and editing variants. Development 138, 4301–4313. [PubMed: 21865324]

Han HA, Cortez MA and Snead OC (2012), Jasper's Basic Mechanisms of the Epilepsies, Bethesda (MD).

Hayashi S and McMahon AP (2002) Efficient recombination in diverse tissues by a tamoxifen-inducible form of Cre. Dev Biol 244, 305–318. [PubMed: 11944939]

Hellwig S, Hack I, Kowalski J, Brunne B, Jarowyj J, Unger A, Bock HH, Junghans D and Frotscher M (2011) Role for Reelin in neurotransmitter release. J Neurosci 31, 2352–2360. [PubMed: 21325502]

Herz J, Goldstein JL, Strickland DK, Ho YK and Brown MS (1991) 39-kDa protein modulates binding of ligands to low density lipoprotein receptor-related protein/alpha 2-macroglobulin receptor. J Biol Chem 266, 21232–21238. [PubMed: 1718973]

Hiesberger T, Trommsdorff M, Howell BW, Goffinet A, Mumby MC, Cooper JA and Herz J (1999) Direct binding of Reelin to VLDL receptor and ApoE receptor 2 induces tyrosine phosphorylation of disabled-1 and modulates tau phosphorylation. Neuron 24, 481–489. [PubMed: 10571241]

Hong SE, Shugart YY, Huang DT, Shahwan SA, Grant PE, Hourihane JO, Martin ND and Walsh CA (2000) Autosomal recessive lissencephaly with cerebellar hypoplasia is associated with human RELN mutations. Nat Genet 26, 93–96. [PubMed: 10973257]

Howell BW, Herrick TM, Hildebrand JD, Zhang Y and Cooper JA (2000) Dab1 tyrosine phosphorylation sites relay positional signals during mouse brain development. Curr Biol 10, 877–885. [PubMed: 10959835]

Huang Y-WA, Zhou B, Wernig M and Südhof TC (2017) ApoE2, ApoE3, and ApoE4 Differentially Stimulate APP Transcription and Aβ Secretion. Cell 168, 427–441.e21. [PubMed: 28111074]

Karbon EW and Enna SJ (1985) Characterization of the relationship between gamma-aminobutyric acid B agonists and transmitter-coupled cyclic nucleotide-generating systems in rat brain. Mol Pharmacol 27, 53–59. [PubMed: 2981401]

Karube F, Kubota Y and Kawaguchi Y (2004) Axon branching and synaptic bouton phenotypes in GABAergic nonpyramidal cell subtypes. J Neurosci 24, 2853–2865. [PubMed: 15044524]

Kawaguchi Y, Karube F and Kubota Y (2006) Dendritic branch typing and spine expression patterns in cortical nonpyramidal cells. Cereb Cortex 16, 696–711. [PubMed: 16107588]

Kuramoto N, Wilkins ME, Fairfax BP, Revilla-Sanchez R, Terunuma M, Tamaki K, Iemata M, Warren N, Couve A, Calver A, Horvath Z, Freeman K, Carling D, Huang L, Gonzales C, Cooper E, Smart TG, Pangalos MN and Moss SJ (2007) Phospho-dependent functional modulation of GABA(B) receptors by the metabolic sensor AMP-dependent protein kinase. Neuron 53, 233–247. [PubMed: 17224405]

Lambert de Rouvroit C and Goffinet AM (1998) The reeler mouse as a model of brain development. Adv Anat Embryol Cell Biol 150, 1–106. [PubMed: 9816727]

Lane-Donovan C, Philips GT, Wasser CR, Durakoglugil MS, Masiulis I, Upadhaya A, Pohlkamp T, Coskun C, Kotti T, Steller L, Hammer RE, Frotscher M, Bock HH and Herz J (2015) Reelin protects against amyloid β toxicity in vivo. Sci Signal 8, ra67. [PubMed: 26152694]

López-Bendito G, Shigemoto R, Kulik A, Paulsen O, Fairén A and Luján R (2002) Expression and distribution of metabotropic GABA receptor subtypes GABABR1 and GABABR2 during rat neocortical development. Eur J Neurosci 15, 1766–1778. [PubMed: 12081656]

Ma YC, Huang J, Ali S, Lowry W and Huang XY (2000) Src tyrosine kinase is a novel direct effector of G proteins. Cell 102, 635–646. [PubMed: 11007482]

Maier PJ, Marin I, Grampp T, Sommer A and Benke D (2010) Sustained glutamate receptor activation down-regulates GABAB receptors by shifting the balance from recycling to lysosomal degradation. J Biol Chem 285, 35606–35614. [PubMed: 20826795]

Miyata T, Nakajima K, Mikoshiba K and Ogawa M (1997) Regulation of Purkinje cell alignment by reelin as revealed with CR-50 antibody. J Neurosci 17, 3599–3609. [PubMed: 9133383]

Mott DD and Lewis DV (1991) Facilitation of the induction of long-term potentiation by GABAB receptors. Science 252, 1718–1720. [PubMed: 1675489]

Nieto M, Monuki ES, Tang H, Imitola J, Haubst N, Khoury SJ, Cunningham J, Gotz M and Walsh CA (2004) Expression of Cux-1 and Cux-2 in the subventricular zone and upper layers II-IV of the cerebral cortex. J Comp Neurol 479, 168–180. [PubMed: 15452856]

Nishikawa M and Kuriyama K (1989) Functional coupling of cerebral ?-aminobutyric acid (GABA) (B) receptor with adenylate cyclase system. Neurochem Int 14, 85–90. [PubMed: 20504404]

Owens DF and Kriegstein AR (2002) Is there more to GABA than synaptic inhibition? Nat Rev Neurosci 3, 715–727. [PubMed: 12209120]

Padgett CL, Lalive AL, Tan KR, Terunuma M, Munoz MB, Pangalos MN, Martínez-Hernández J, Watanabe M, Moss SJ, Luján R, Lüscher C and Slesinger PA (2012) Methamphetamine-evoked depression of GABA(B) receptor signaling in GABA neurons of the VTA. Neuron 73, 978–989. [PubMed: 22405207]

Palop JJ and Mucke L (2016) Network abnormalities and interneuron dysfunction in Alzheimer disease. Nat Rev Neurosci 17, 777–792. [PubMed: 27829687]

Pinard A, Seddik R and Bettler B (2010) GABAB receptors. Adv Pharmacol 58, 231–255. [PubMed: 20655485]

Pohlkamp T, Dávid C, Cauli B, Gallopin T, Bouché E, Karagiannis A, May P, Herz J, Frotscher M, Staiger JF and Bock HH (2014) Characterization and distribution of Reelin-positive interneuron subtypes in the rat barrel cortex. Cereb Cortex 24, 3046–3058. [PubMed: 23803971]

Sakaba T and Neher E (2003) Direct modulation of synaptic vesicle priming by GABA(B) receptor activation at a glutamatergic synapse. Nature 424, 775–778. [PubMed: 12917685]

Terunuma M, Pangalos MN and Moss SJ (2010) Functional modulation of GABAB receptors by protein kinases and receptor trafficking. Adv Pharmacol 58, 113–122. [PubMed: 20655480]

Terunuma M, Vargas KJ, Wilkins ME, Ramírez OA, Jaureguiberry-Bravo M, Pangalos MN, Smart TG, Moss SJ and Couve A (2010) Prolonged activation of NMDA receptors promotes dephosphorylation and alters postendocytic sorting of GABAB receptors. PNAS 107, 13918–13923. [PubMed: 20643948]

Trommsdorff M, Gotthardt M, Hiesberger T, Shelton J, Stockinger W, Nimpf J, Hammer RE, Richardson JA and Herz J (1999) Reeler/Disabled-like disruption of neuronal migration in knockout mice lacking the VLDL receptor and ApoE receptor 2. Cell 97, 689–701. [PubMed: 10380922]

Wagener RJ, Dávid C, Zhao S, Haas CA and Staiger JF (2010) The somatosensory cortex of reeler mutant mice shows absent layering but intact formation and behavioral activation of columnar somatotopic maps. J Neurosci 30, 15700–15709. [PubMed: 21084626]

Weir K, Blanquie O, Kilb W, Luhmann HJ and Sinning A (2014) Comparison of spike parameters from optically identified GABAergic and glutamatergic neurons in sparse cortical cultures. Front Cell Neurosci 8, 460. [PubMed: 25642167]

Welt C and Steindler DA (1977) Somatosensory cortical barrels and thalamic barreloids in reeler mutant mice. Neuroscience 2, 755–766. [PubMed: 593554]

Willnow TE, Rohlmann A, Horton J, Otani H, Braun JR, Hammer RE and Herz J (1996) RAP, a specialized chaperone, prevents ligand-induced ER retention and degradation of LDL receptor-related endocytic receptors. EMBO J 15, 2632–2639. [PubMed: 8654360]

Xiao M-F, Xu D, Craig MT, Pelkey KA, Chien C-C, Shi Y, Zhang J, Resnick S, Pletnikova O, Salmon D, Brewer J, Edland S, Wegiel J, Tycko B, Savonenko A, Reeves RH, Troncoso JC, McBain CJ, Galasko D and Worley PF (2017) NPTX2 and cognitive dysfunction in Alzheimer's Disease. eLife 6.

Xu J and Wojcik WJ (1986) Gamma aminobutyric acid B receptor-mediated inhibition of adenylate cyclase in cultured cerebellar granule cells. J Pharmacol Exp Ther 239, 568–573. [PubMed: 2430096]

Yuste R, MacLean J, Vogelstein J and Paninski L (2011) Imaging action potentials with calcium indicators. Cold Spring Harb Protoc 2011, 985–989. [PubMed: 21807854]

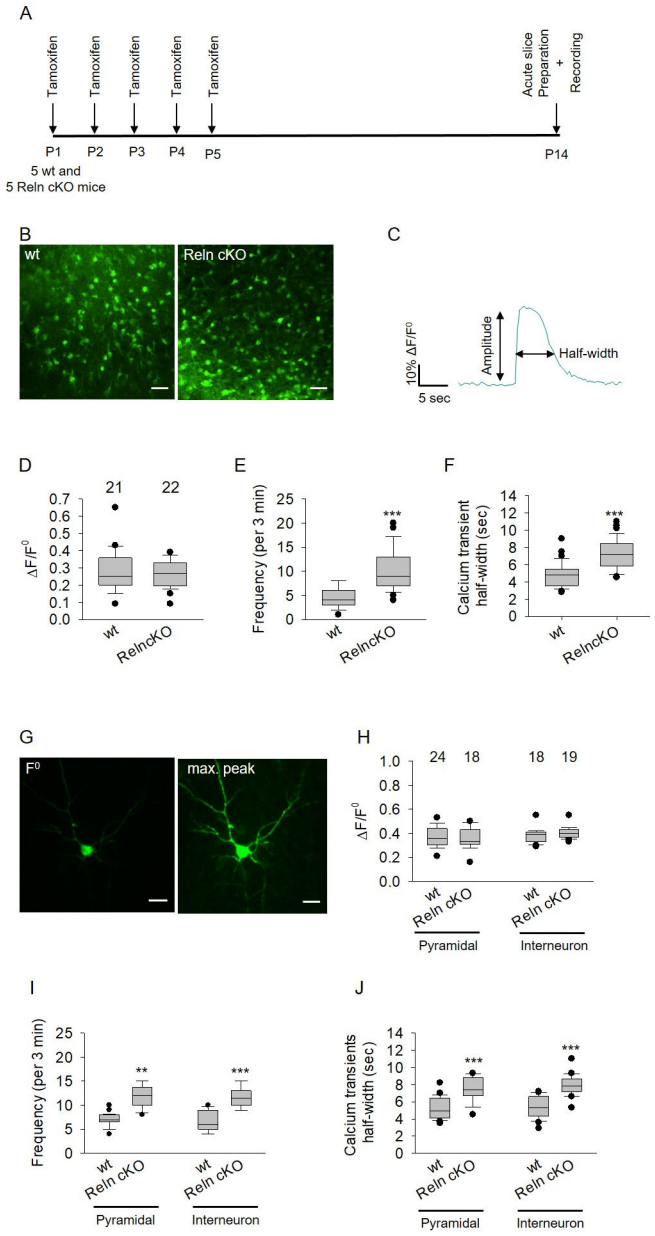

Fig. 1. Recording of neuronal activity in Reln^{cKO} mice.

(A) Graphical flow chart of experimental procedures. In each experiment, slices were prepared from 5 wt and 5 Reln^{cKO} mice. (B): Confocal image examples of OGB-1 AM loaded P14 acute neocortical wt and Reln^{cKO} slices. Scale bars: 20 μm. (C): Typical example of spike waveform from a recorded cell which shows amplitude and Ca^{+2} transient (spike) half-width. (D): The box-plot in the graph represents the values of maximal increase in Ca^{2+}-signal amplitude in control wt and Reln^{cKO} acute slices expressed as $\Delta F/F^0$, which is unaltered. (E): The Ca^{2+} frequency is significantly higher in the Reln^{cKO} when compared to wt, and (F) the Ca^{+2} transient half-width is significantly higher in Reln^{cKO} when compared to wt. Mann–Whitney U test; ***P<0.001. The number of acute slices analysed is indicated above the box-plots in (D). To assess pyramidal cells and interneurons separately, acute

slices were transfected with GCaMP6s plasmid to visualize the cell type (G-J). (G): Confocal images of a GCaMP6s transfected pyramidal cell in a wt P14 acute neocortical slice during Ca^{2+}-imaging at resting fluorescence (F^0) and at maximal amplitude peak. Scale bars: 20 μm. (H): The box-plot in the graph shows no change in maximal Ca^{2+}-amplitude signals between control wt and $Reln^{cKO}$ groups for both cell types, but shows (I and J) a significant increase in Ca^{2+} frequency and Ca^{+2} transients half-width in $Reln^{cKO}$ recorded slices in comparison to wt for both pyramidal cells and interneurons. One-way ANOVA on Ranks followed by Dunn's Multiple Comparison Test, ***$p < 0.001$ and **$P<0.01$. The number of single cells in (H-J) is indicated above the box-plots in (H). The data is obtained from 3 independent acute slice preparations.

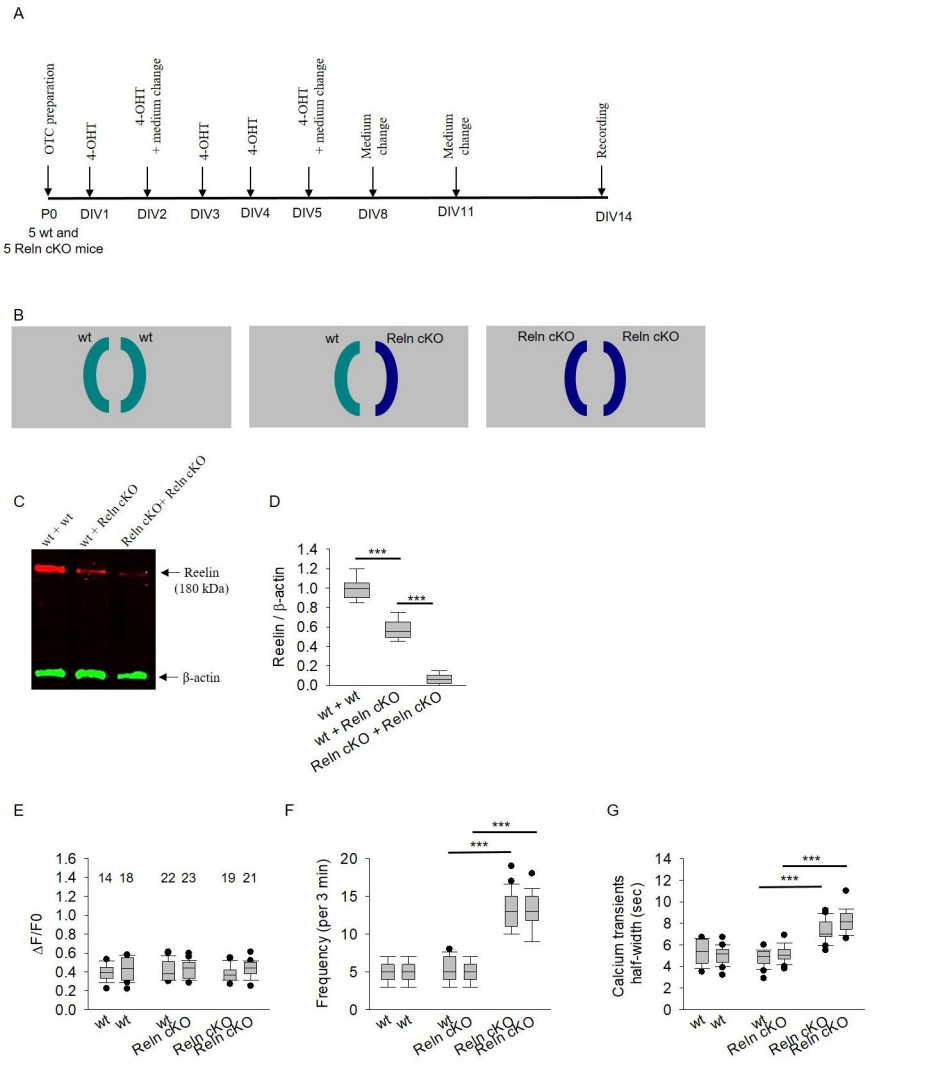

Fig. 2. Secreted Reelin rescues impaired Ca^{2+}-frequency in $Reln^{cKO}$ OTCs.

(A) A graphical flow chart for OTCs experimental procedure. (B) Schematic representation of the co-culture experimental approach. Left: Two co-cultured wt OTCs. Middle: A wt OTC co-cultured together with a $Reln^{cKO}$ OTC. Right: Two co-cultured $Reln^{cKO}$ OTCs. (C) Co-culture medium lysates from DIV14 OTCs (40 OTCs obtained from 5 mice for each experimental group) were analysed by western blot. (D) Quantification of the western blot 180-kDa Reelin signals. An actin antibody was used as loading control. The densiometric quantification showed a decreased Reelin protein level in the wt + $Reln^{cKO}$ co-culture medium and almost complete absence in the $Reln^{cKO}$ + $Reln^{cKO}$ co-culture medium. One-way ANOVA followed by Holm-Sidak Multiple Comparison Test, ***$p < 0.001$ wt + $Reln^{cKO}$ compared to wt + wt; ***$P<0.001$ wt + $Reln^{cKO}$ compared to $Reln^{cKO}$ + $Reln^{cKO}$. At 14 DIV, OTCs were loaded with OGB-1 AM and recorded. (E) The box-plot in the graph represents the values of maximal increase in Ca^{2+} signal amplitude, which shows no change in all experimental groups. (F and G) The box-plot shows a significant increase in Ca^{2+} frequency and Ca^{+2} transient half-width in $Reln^{cKO}$ co-cultured OTCs. Note that the enhanced frequency and Ca^{+2} transients half-width observed in the $Reln^{cKO}$ OTC are

restored to a normal level when it is co-cultured together with a wt OTC. The number of recorded OTC is indicated above the box-plots in (E). One-way ANOVA on Ranks followed by Dunn's Test, ***$p < 0.001$. The data is obtained from 3 independent OTCs preparations.

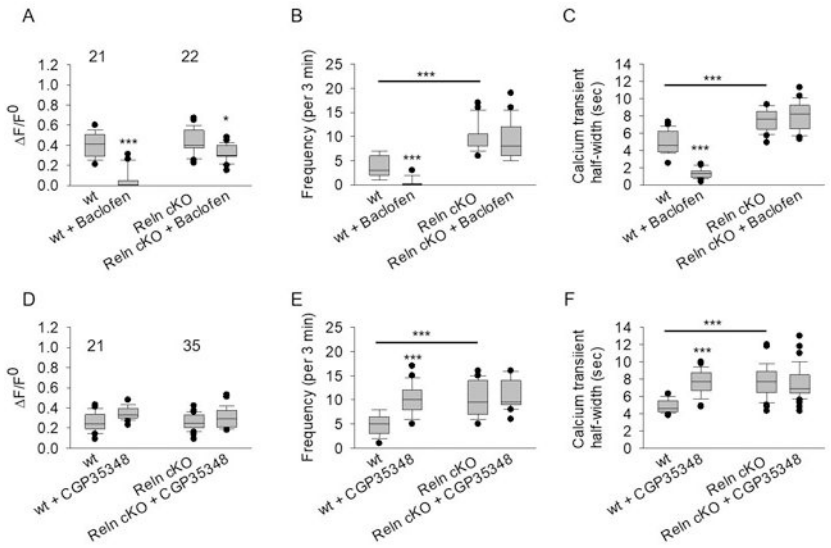

Fig. 3. $GABA_BRs$ are dysfunctional in $Reln^{cKO}$.

To test the functionality of the $GABA_BRs$ at DIV14, OTCs were loaded with OGB-1 AM, spontaneous activity was first recorded and then the $GABA_BR$ agonist baclofen (10 μm) was added. In each experiment, OTCs were prepared from 5 wt and 5 $Reln^{cKO}$ mice. (A): The application of baclofen immediately activates $GABA_BRs$ and thereby strongly decreases Ca^{+2} amplitude in wt OTCs (One-way ANOVA on Ranks followed Tukey's Test, ***$p < 0.001$) but to a lesser extent in $Reln^{cKO}$ OTCs (*$p < 0.05$). Ca^{2+}-frequency (B) and Ca^{2+} transient half-width (C) were significantly decreased in the wt but not in $Reln^{cKO}$ OTCs (One-way ANOVA on Ranks followed Tukey's Test, ***$p < 0.001$). The $GABA_BR$ antagonist CGP35348 (10 μM) did not alter Ca^{2+} amplitudes in both wt and $Reln^{cKO}$ OTCs (D). The application of CGP35348 significantly enhanced Ca^{2+} frequency (E) and Ca^{2+} transient half-width (F) in wt but not $Reln^{cKO}$ OTCs. One-way ANOVA on Ranks followed by Dunn's Test, ***$p < 0.001$. The number of OTCs analysed is indicated above the box-plot in (D). The data is obtained from 3 independent OTCs preparations.

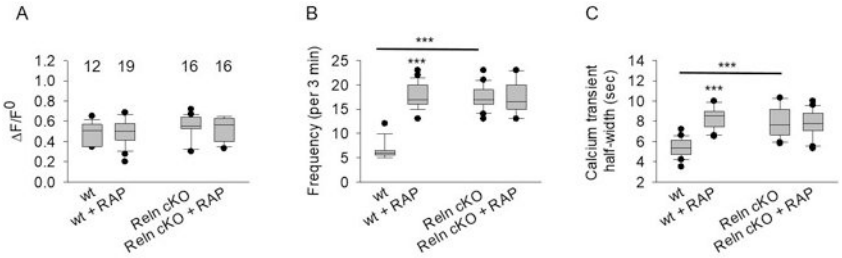

Fig. 4. Effect of chronic blockade with the LDL-receptor chaperone RAP.

$Reln^{cKO}$ or wt OTCs chronically treated with RAP (50 μg) were loaded with OGB-1 AM and recorded. In each experiment, OTCs were prepared from 5 wt and 5 $Reln^{cKO}$ mice. Control wt or $Reln^{cKO}$ OTCs were treated with H_2O. (A) RAP blockade did not affect Ca^{2+}-amplitude in wt and $Reln^{cKO}$ OTCs. However, RAP significantly increased Ca^{2+}-frequency (B) and Ca^{2+}-transient half-width (C) in wt but not $Reln^{cKO}$ OTCs. One-way ANOVA on Ranks followed by Dunn's Test, ***$p < 0.001$. The number of OTCs analysed is indicated above the box-plots in (A). The data is obtained from 3 independent OTCs preparations.

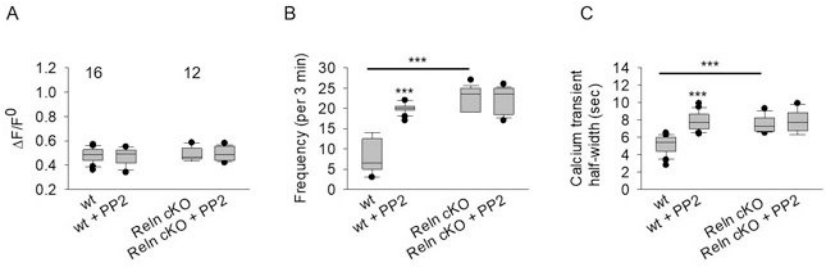

Fig. 5. Effect of acute Src kinase inhibition on wt and Reln^{cKO} Ca^{2+} activity.

Acute application of PP2 (1 μM) did not affect Ca^{2+}-amplitude in both wt and Reln^{cKO} OTCs (A). However, PP2 application enhances Ca^{2+} frequency (B) and Ca^{2+} transient half-width (C) in wt but not Reln^{cKO} OTCs (B). In each experiment, OTCs were prepared from 5 wt and 5 Reln^{cKO} mice. One-way ANOVA on Ranks followed by Dunn's Test, ***$p < 0.001$. The number of OTCs analysed is indicated above the box-plots. The data is obtained from 3 independent OTCs preparations.

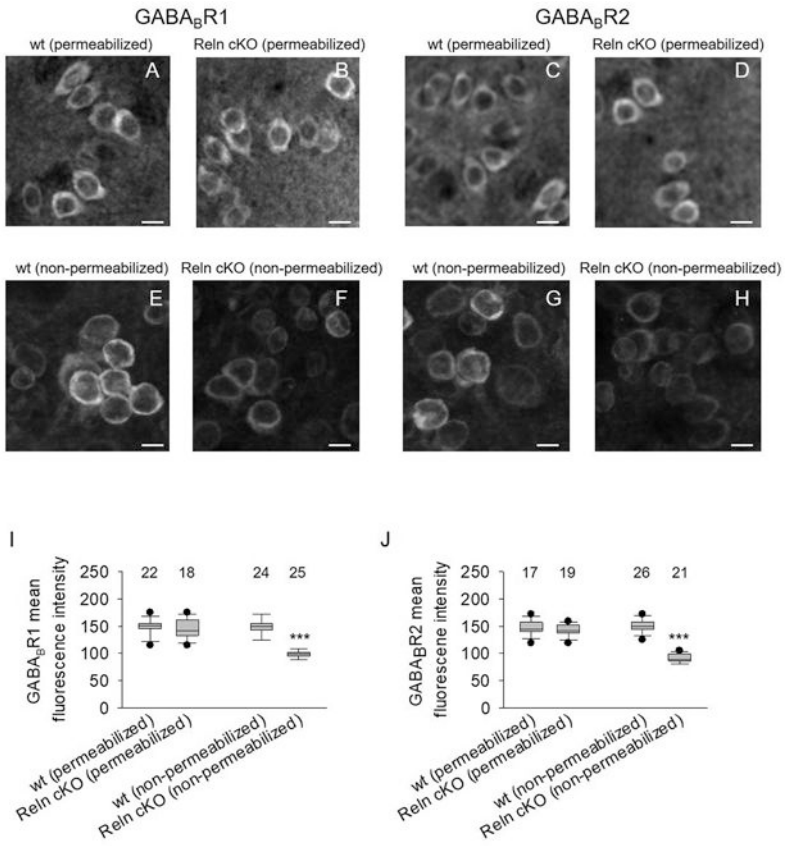

Fig. 6. Surface GABA$_B$R1 and GABA$_B$R2 expression are reduced in the Reln^{cKO} slices.

Acute slices (P14) from wt and Reln^{cKO} mice were immunostained against total (permeabilized) and surface (non-permeabilized) GABA$_B$R1 and GABA$_B$R2 expression. In each experiment, slices were prepared from 5 wt and 5 RelncKO mice. Confocal image example at 40 x magnification from layers II/III somatosensory cortices of wt (A) and Reln^{cKO} (B) acute slices stained against GABA$_B$R1 or GABA$_B$R2 (C and D) under permeabilization condition to detect total receptor expression. Confocal image example of wt (E) and Reln^{cKO} (F) acute slices stained against GABA$_B$R1 or GABA$_B$R2 (G and H) under non-permeabilization condition for receptor surface expression. (I) The box-plots represent values of average pixel intensity of total (permeabilized) and surface (non-permeabilized) GABA$_B$R1 expression. (J) The box-plots represent values of average pixel intensity of total (permeabilized) and surface (non-permeabilized) GABA$_B$R2 expression. One-way ANOVA on Ranks followed by Dunn's Test, ***$p < 0.001$. The number of acute slices analysed is indicated above the box-plots. The data is obtained from 3 ex-vivo acute slice preparations. Scale bar: 10 μm.

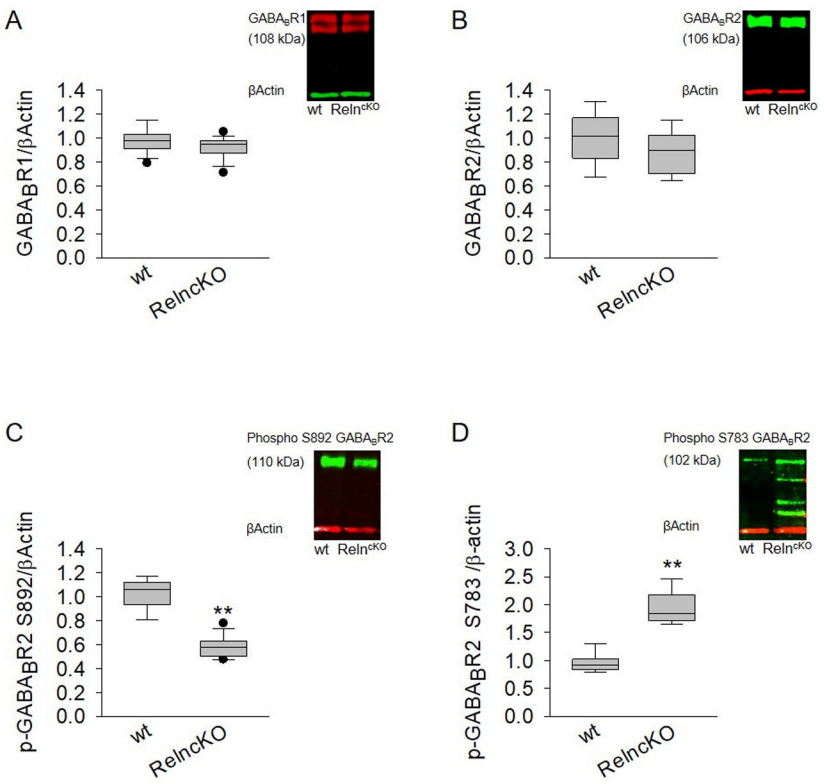

Fig. 7. Reelin signaling regulates GABAB-receptor phosphorylation.

Cortical lysates from P14 wt and Reln^{cKO} mice were analysed by western blot (n = 6 animals from each group; The data is obtained from 3 different tissue explants). Total GABA$_B$R1 (A) and GABA$_B$R2 (B) were unaltered in Reln^{cKO} in comparison to wt control. (C): Phosphorylation of GABA$_B$R2 at S892 was significantly reduced in Reln^{cKO} (T-test, ***$p < 0.001$), whereas phosphorylation at S783 was significantly increased (D) when compared to wt (T-test, ***$p < 0.001$), and appearance of several bands suggests proteolysis of the receptor (Gassmann and Bettler 2012; Maier et al. 2010).